Journal of Civil and Hydraulic Engineering
https://www.acadlore.com/journals/JCHE

Geophysical Evaluation of Subsurface Structural Characteristics for Dam Site Selection in the Garko Area, Wudil Sheet 81 SE, Northern Nigeria Using Aeromagnetic Data

Mubarak Abubakar[1*], Maruf Abiola Agbaje[2], Rahama Tijjani Darma[3], Adamu Muhammad[4]

[1] Department of Geology, Kano University of Science and Technology, 713223 Wudil, Nigeria
[2] Department of Marine Sciences, University of Georgia, 30602 Athens, United States
[3] Department of Geology, Bayero University, 700241 Kano, Nigeria
[4] School of Earth Resources, China University of Geosciences, 430074 Wuhan, China

[*] Correspondence: Mubarak Abubakar (Mubarakabubakarbnk@gmail.com)

Received: 10-11-2025 **Revised:** 12-08-2025 **Accepted:** 12-16-2025

Citation: M. Abubakar, M. A. Agbaje, R. T. Darma, and A. Muhammad, "Geophysical evaluation of subsurface structural characteristics for dam site selection in the Garko Area, Wudil Sheet 81 SE, Northern Nigeria using aeromagnetic data," *J. Civ. Hydraul. Eng.*, vol. 3, no. 4, pp. 231–244, 2025. https://doi.org/10.56578/jche030405.

Abstract: The suitability of the Garko area (Wudil Sheet 81 SE) for dam construction has been assessed through the analysis of aeromagnetic data with a spatial resolution of 500 m line spacing and a flight altitude of 80 m. The investigation, conducted in north-central Nigeria, aimed to delineate subsurface structural features and identify magnetic anomalies relevant to dam site selection. The integration of quantitative filtering techniques with magnetic interpretation significantly improved the reproducibility and reliability of the geophysical site evaluation process, thereby enhancing the accuracy of the assessment for sustainable dam development. The Total Magnetic Intensity (TMI) data was processed using upward continuation at a height of 1 km, with the resulting dataset serving as the primary input for the analysis. Several edge detection methods and interpretation techniques were employed, including the Gaussian filter (cut-off frequency of 0.05 cycles/km), Reduce to Pole (RTP) (for low latitudes), and Tilt Derivatives filters, to delineate structural trends and boundary zones. From the TMI data derived from the Tilt Derivative map, three magnetic zones were identified: a low magnetic intensity zone (LM) with an amplitude range of -1.4 to -0.3 nT, a moderate magnetic zone (MM) with amplitudes ranging from -0.3 to 0.4 nT, and a high magnetic intensity zone (HM) with amplitudes from 0.4 to 1.3 nT. These zones were represented by color codes from blue to pink, corresponding to the magnetic amplitude values. Lineament analysis conducted on the Tilt Derivative map revealed prominent NE–SW and NW–SE structural trends, which are believed to control subsurface drainage and fracture systems. Areas characterized by low magnetic intensities and sparse lineament density were identified as geologically stable, suggesting their suitability for the foundation of a dam. This study demonstrates that magnetic data, when combined with advanced geophysical techniques, can play a pivotal role in site selection for sustainable infrastructure development.

Keywords: Dam; Aeromagnetic; Remote sensing; Geological mapping; Structural trends

1 Introduction

Dams represent some of the most significant and large-scale structures in civil engineering, with a long life expectancy and substantial importance in water resource management. However, due to geological, hydrological, and topographic constraints, the availability of ideal dam sites is limited. These structures are designed and constructed to serve vital purposes, including water storage for irrigation, flood control, and hydroelectric power generation. The design of a dam must therefore ensure long-term stability and durability. Among the various factors influencing dam design, the geological conditions of the site are of paramount importance, as they govern both the foundation characteristics and the materials available for construction [1, 2].

Water resource development is increasingly critical in addressing growing demands for domestic, agricultural, and industrial use, particularly in semi-arid regions such as Northern Nigeria. Dams have been identified as an effective strategy for managing seasonal water availability, ensuring irrigation, and mitigating floods. However, the suitability of a dam site is predominantly determined by the geological, structural, and geophysical characteristics of the underlying terrain. Thus, a thorough understanding of subsurface structures is essential for the safe, sustainable, and cost-effective development of dam infrastructure [3, 4].

In recent years, geophysical methods, particularly magnetic surveys, have found broad application in civil engineering and hydrological studies due to their efficacy in detecting subsurface features, such as fractures, faults, and lithological contacts. These features significantly influence groundwater flow and rock stability, factors that are critical in determining suitable locations for dam construction. The magnetic method, in particular, is sensitive to variations in the magnetic properties of rocks and can identify concealed geological structures that are not readily observable at the surface [5, 6].

The Garko area, located within Wudil Sheet 81 SE in Northern Nigeria, forms part of the Basement Complex terrain, which is composed of crystalline rocks such as migmatites, granites, and schists. The region has historically suffered from water scarcity due to erratic rainfall patterns and inadequate surface water retention. As a result, identifying geologically suitable zones for dam construction in the area is a crucial and timely endeavor. The region's structural complexity, dominated by faults, joints, and fractures, necessitates a detailed geophysical investigation to identify zones with stable bedrock and optimal water retention capacity [4].

This study employs aeromagnetic data interpretation techniques to identify magnetic lineaments, which serve as proxies for subsurface structural features. These lineaments are analyzed alongside geological maps and terrain characteristics to delineate potential zones for dam construction. The primary objective of the study is to integrate geophysical data with structural and lithological information to propose feasible dam sites that will ensure structural integrity, water security, and long-term sustainability.

Several studies have applied geophysical and geotechnical techniques to evaluate proposed dam foundations in Nigeria. Aina et al. [7] demonstrated the utility of such methods in assessing the suitability of dam sites. More recent studies have emphasized the power of aeromagnetic filtering techniques to delineate structural trends that govern groundwater flow and rock competence, which are essential for selecting viable dam sites [8]. However, there is a noticeable gap in the literature regarding the systematic application of high-resolution aeromagnetic filtering combined with quantitative lineament analysis for dam-site zoning in the Kano region [9].

This study addresses this gap by integrating several aeromagnetic data processing techniques, including RTP, Gaussian filters, and Tilt Derivatives, with lineament mapping to identify structurally stable zones for dam construction in the Garko area. These techniques are employed to reveal subsurface features that influence the stability of potential dam sites, with the aim of providing a robust framework for dam-site selection in geologically complex terrains. The findings are expected to support more informed decision-making in the planning and design of small to medium-scale dams in Northern Nigeria, where subsurface data are often limited.

1.1 Study Area

Garko Local Government Area (LGA) is located in the southeastern part of Kano State, Northern Nigeria, within the tropical savanna (Aw) climatic zone of Köppen's classification. The climate is characterized by a distinct wet season from May to September and a prolonged dry season from October to April, influenced by the seasonal migration of the Inter-Tropical Discontinuity (ITD). Mean annual rainfall ranges from 800 mm to 1,000 mm, while temperatures range from 26°C to 38°C, with peak values recorded in March and April [10, 11].

The study area includes Indabo, Lamire, Sayasaya, Acika, Darki, Faragai, Sarina, Kafin Malamai, Garin Ali, Garfa, Sulaila, and Garko LGA in the southwestern part of Kano State, within Wudil Sheet 81 SE of Northwestern Nigeria. It lies between latitudes $11°30'00''$ N and $11°44'00''$ N, and longitudes $8°46'00''$ E and $9°00'00''$ E, with an estimated total area of about 678 km^2 at a map scale of 1:50,000 [12, 13].

The Garko area is geographically bordered by Wudil and Gaya to the south, Sumaila and Takai to the north, Kibiya to the east, and Rano and Bunkure to the west [12]. The area is accessible via several motorable roads from Garko, including the Kano–Wudil–Duru road, Wudil–Kafin Malamai road, and Garko–Sumaila road. There is also a network of footpaths throughout the area, with nearly 75% of access provided by footpaths [13], as shown in Figure 1.

Hydrologically, Garko LGA is traversed by several ephemeral streams and surface channels that form part of the Hadejia–Jama'are River Basin system, contributing to seasonal runoff and groundwater recharge processes in the region [14]. These streams typically exhibit high discharge during the rainy season and little to no flow during the dry season, which makes the area suitable for hydrological interventions, including small- and medium-scale dams for water supply and irrigation.

Geomorphologically, the terrain consists of gently undulating plains with elevations ranging from 400 m to 520 m above sea level, typical of the Northern Nigerian Basement Complex landscape. The surface is primarily composed of lateritic soils and regolith materials, while the subsurface geology is dominated by Precambrian Basement Complex rocks, including migmatite–gneiss complexes, granites, schists, and quartzites [15, 16]. Structural elements such as fractures, joints, and faults strongly influence drainage and subsurface water movement, making them critical factors in dam-site selection [17].

The combination of climatic variability, seasonal hydrology, moderate relief, and structurally complex basement geology makes Garko LGA a suitable candidate for evaluating dam-site suitability through the use of high-resolution aeromagnetic data.

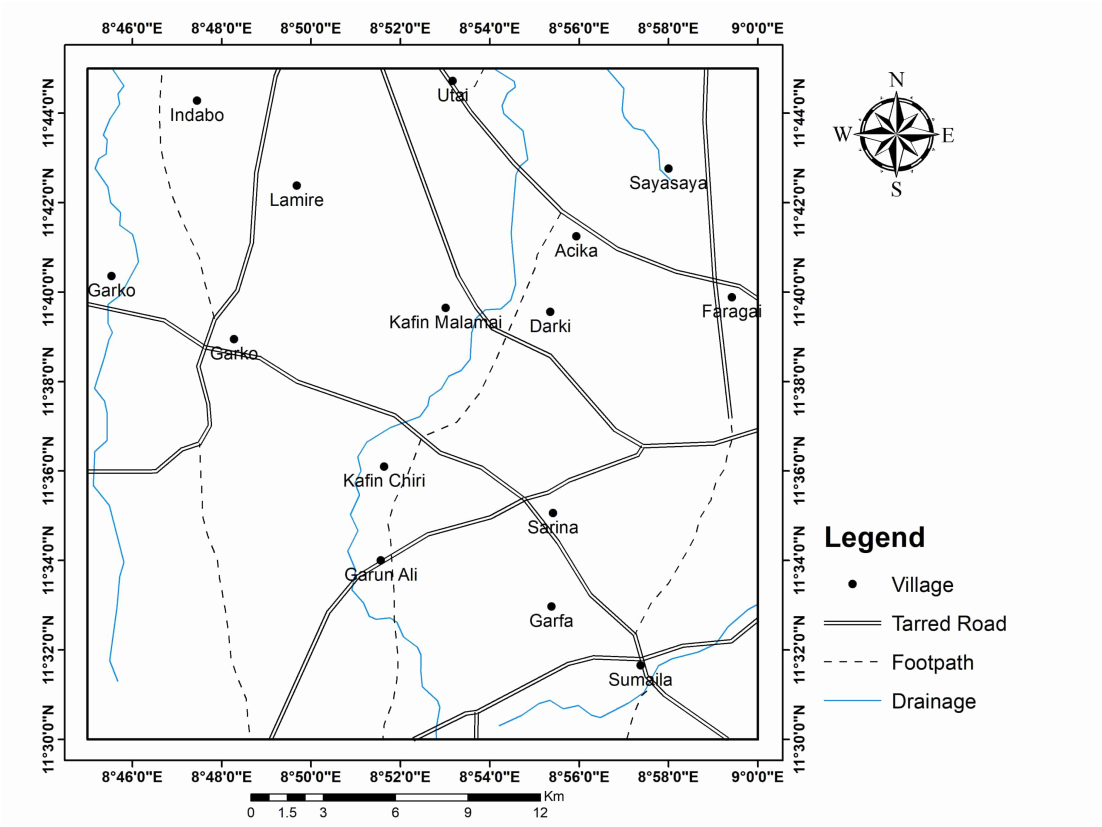

Figure 1. Location map of the study area for accessibility (Modified after NGSA)

1.2 Geological Setting

The study area, Garko LGA, lies within the Precambrian Basement Complex of Northern Nigeria, which forms part of the Pan-African mobile belt situated between the West African and Congo Cratons [15, 17]. The Basement Complex is composed predominantly of migmatite–gneiss complexes, schist belts, and younger Granite intrusions, each with distinctive lithological and magnetic characteristics.

The migmatite gneiss complex, which represents the oldest rock unit, is characterized by alternating bands of quartz, feldspar, and ferromagnesian minerals. These rocks typically exhibit moderate to high magnetic susceptibility due to the presence of biotite, hornblende, and magnetite grains, resulting in relatively high TMI values on aeromagnetic maps [17–19].

The schist belts, composed mainly of metasedimentary and metavolcanic rocks such as quartzite, phyllite, and amphibolite, show variable magnetic responses. Amphibolites and metavolcanic rocks generally produce anomalously high magnetic signals due to their mafic mineral content, whereas quartzites and phyllites are comparatively magnetically quiet [20].

In contrast, the Younger Granites and granitoid intrusions, composed primarily of quartz, feldspar, and minor biotite, are magnetically subdued because of their low ferromagnetic mineral concentration. Their emplacement, however, often causes magnetic discontinuities that are useful in delineating fault zones and intrusive contacts.

These lithological variations play a crucial role in aeromagnetic interpretation, as differences in rock magnetization help in identifying subsurface structures such as lineaments, faults, shear zones, and intrusive boundaries that are essential for dam-site investigations. In the Garko area, the contrast between the high magnetic signatures of the migmatite gneiss complex and the low magnetic signatures of granitic intrusions provides an effective means of mapping structural controls relevant to groundwater and dam construction potential.

Tectonically, these rocks have undergone multiple phases of deformation, including faulting, metamorphism, and folding during the Pan-African Orogeny, approximately 600 million years ago [15, 19]. The lineaments mapped in the area trend mainly ENE–WSW, followed by WNW–ESE, with some NE–SW, NNE–SSW, and NNW–SSE trends (Figure 2) [17, 21].

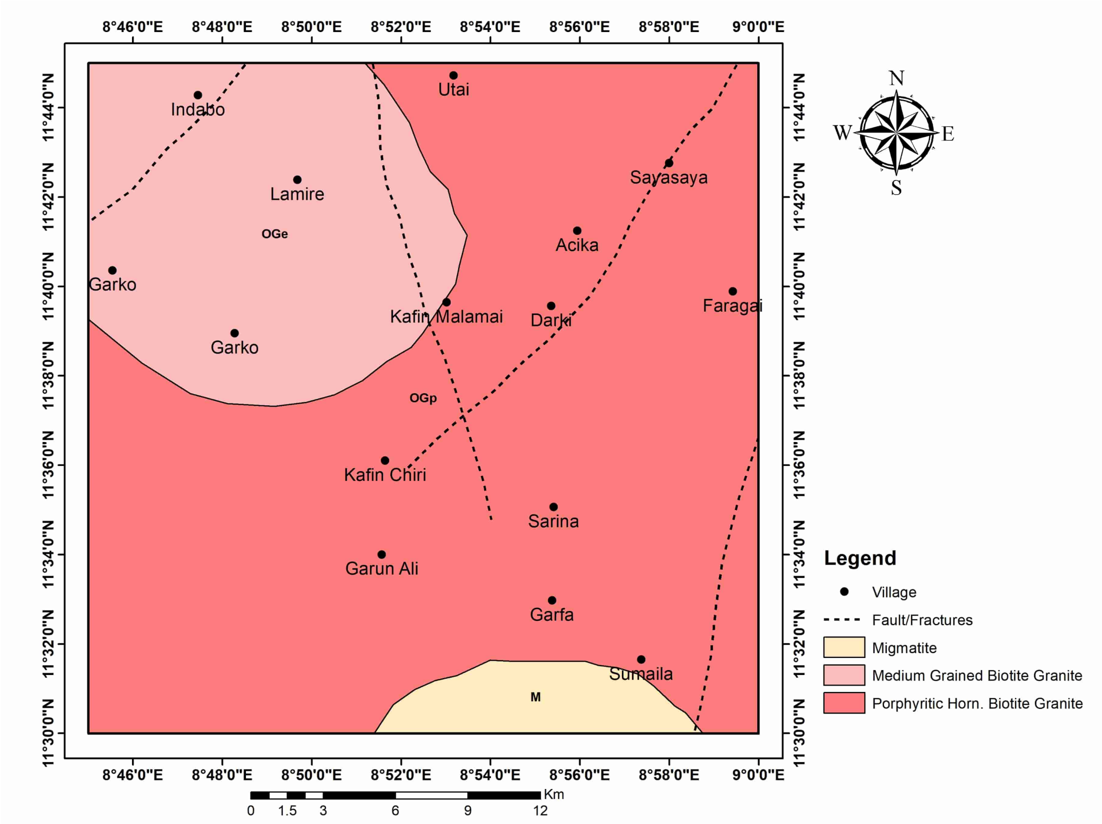

Figure 2. Geological map of study area (Modified after NGSA)

2 Materials and Method

The use of software where applicable involved Oasis Montaj, Global Mapper, ArcGIS, Microsoft Office, Georose, and a personal laptop computer as materials for this research, applied to an aeromagnetic geophysical data set of the Southeastern part of Wudil Sheet 81. The aeromagnetic data was collected from the Nigerian Geological Survey Agency [22] headquarters, and subsequently processed using the above-mentioned software packages.

Geosoft's Oasis Montaj software platform is widely used for working with large volumes of spatial data and provides the functionality required to manage, manipulate, visualize, and map Earth Science data [23, 24]. Global Mapper, developed by Blue Marble Geographics, was used to geo-reference and create the boundary around the magnetic anomaly map [25]. Similarly, ArcGIS software [26] was used to analyze, edit, digitize, and create the final magnetic lineament (structural) map.

The aeromagnetic maps used for the study were acquired from NGSA [22] as part of the high-resolution aeromagnetic survey of Nigeria. The data were obtained at a nominal flight height of 80 m along N–S flight lines spaced at 500 m using advanced magnetometric equipment, producing higher-resolution results than earlier datasets [27, 28]. The geomagnetic gradient was removed using the International Geomagnetic Reference Field (IGRF) correction method to obtain the TMI maps [29, 30].

An aeromagnetic survey is a standard geophysical method that employs a magnetometer to measure the Earth's magnetic field aboard an aircraft [31, 32]. This technique, first applied in World War II for submarine detection, remains widely used for geological and resource investigations [33]. As the aircraft flies, the magnetometer records the total magnetic field intensity, comprising both the Earth's natural field and variations from temporal effects such as solar winds or aircraft-induced interference. By subtracting these effects, the resulting magnetic maps reveal the distribution of magnetic minerals, most commonly magnetite, within the Earth's crust [34, 35].

Since rock types vary in their magnetic properties, aeromagnetic maps provide valuable insight into subsurface geological structures, fault systems, and folds [27, 30]. Today, aeromagnetic data are often visualized using color-coded or shaded computer-generated images that highlight anomalies, rather than traditional contour plots [28, 32].

2.1 Procedure for Lineament Extraction

The steps followed in data processing are summarized in Figure 3. The linking arrows in the diagram illustrate the sequential processes leading to the final extracted lineament (structural) map.

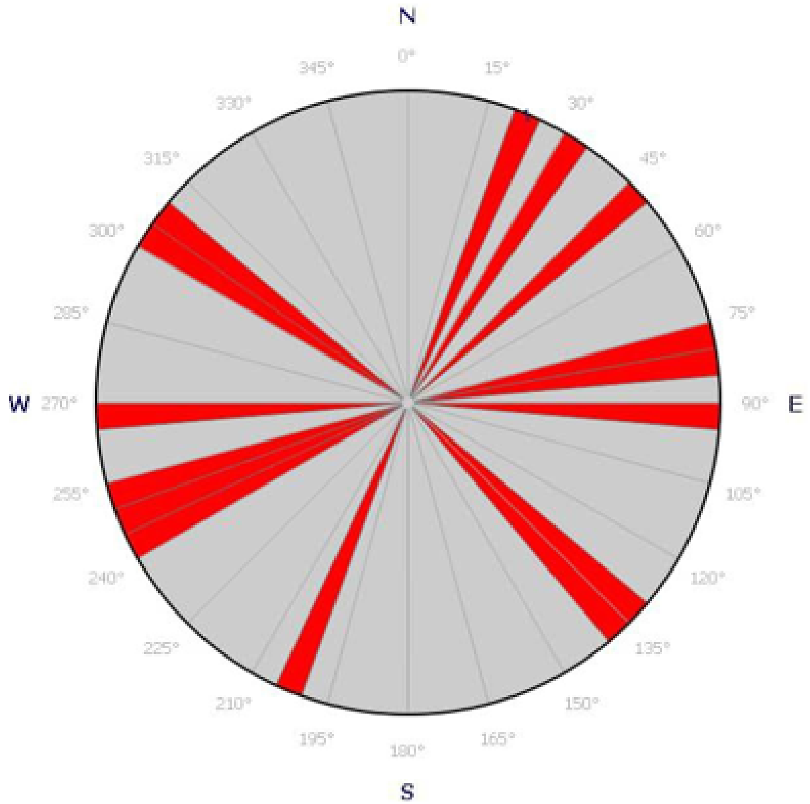

Figure 3. Rose diagram of the study area from Wudil Sheet 81 SE

2.2 Magnetic Intensity Data

The raw aeromagnetic dataset containing TMI values and coordinates was obtained from NGSA [22]. These were imported into Oasis Montaj v6.4.2 for quality control and preprocessing [23, 24].

2.3 2D Magnetic Maps

Within Oasis Montaj, the unprocessed TMI map was imported, and the database containing TMI values and coordinates was gridded. After error-checking and quality validation, the TMI values served as inputs for inversion and filtering algorithms. Different filtering techniques such as Gaussian filters, RTP, Tilt Derivative, and First Vertical Derivative (FVD) were applied to enhance geological features [33, 34].

2.4 Boundary Mapping and Map Completion

Global Mapper was employed to delineate the study boundary and grid extent [25]. The completed data were exported as shapefiles and subsequently imported into ArcGIS for cartographic finishing. At this stage, the lineament map was finalized by adding essential cartographic elements, including boundary outlines, scale, north arrow, grid, and legend [26].

Lineament mapping is the process of tracing and interpreting linear features that represent faults, fractures, or lithological boundaries. Such mapping is often performed on geophysical datasets (e.g., aeromagnetic data), DEMs, radar, and satellite images [29, 35]. Interpreted lineaments provide insights into structural geology, groundwater exploration, and dam site suitability studies [30, 34].

3 Result

The results obtained from 2D magnetic anomaly maps and the magnetic lineament map of Wudil SE sheet 81, Northwest Nigeria, derived from four filtering techniques, are presented in Figures 4–8, while the final digitization of the lineament map is presented in Figure 9 and Figure 10. In this study, digital filters such as Gaussian, RTP, and Tilt Derivative were used to evaluate magnetic anomalies within the study area, consistent with previous geophysical filtering approaches [36, 37]. The results obtained from Oasis Montaj, Global Mapper, and ArcGIS software were combined to generate the magnetic lineament intensity maps.

The interpretation of the generated maps is exclusively qualitative. Zones were analyzed through visual inspection of the magnetic lineament maps, using the color scale and corresponding magnetic intensity (MI) values. Generally, the color codes, which range from blue through green to pink, represent low, medium, and high magnetic intensity values, respectively.

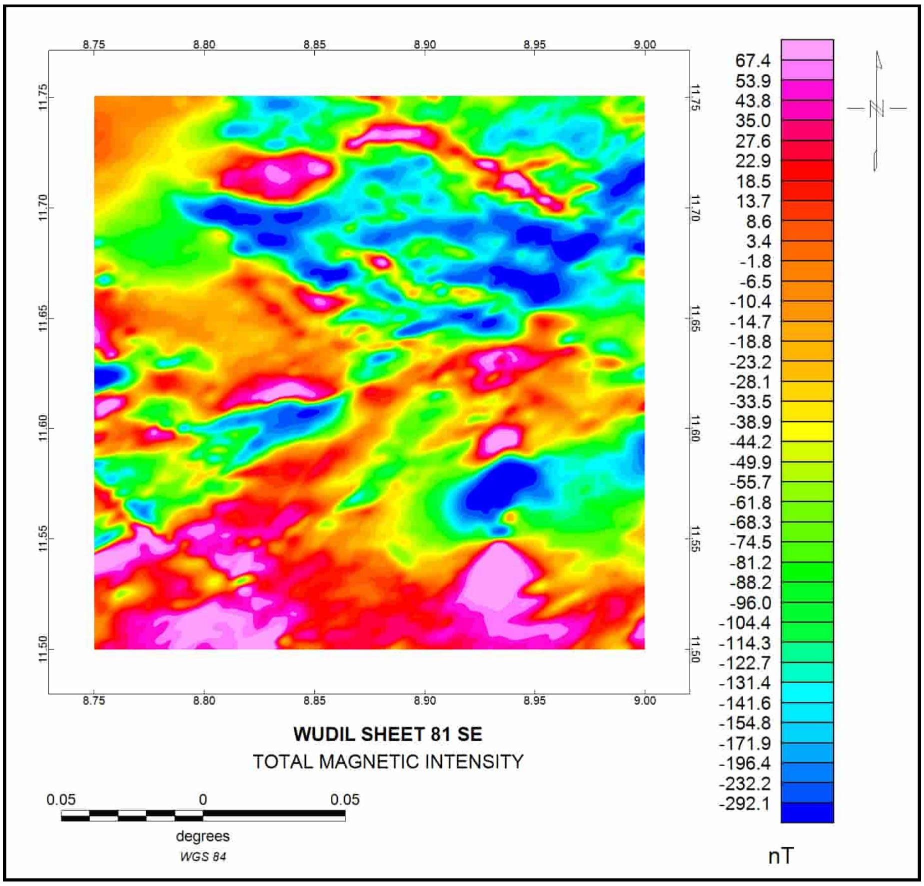

Figure 4. Total intensity map from Wudil Sheet 81SE

3.1 TMI and Filtering Technics

Figure 4 presents the unprocessed TMI map as obtained from NGSA. The TMI values range from 67.4 nT to -292.1 nT, with zones of high magnetic intensity (67.4 to -44.2 nT) indicated using pink to yellow colors, and low intensity zones (-49.9 to -292.1 nT) shown in green to blue. Interpretation of the raw TMI map is limited, as residual anomalies of interest are not yet separated from the regional field. Similar challenges in direct TMI interpretation have been noted in aeromagnetic studies [36].

3.1.1 Gaussian filter

The Gaussian filter, which includes both high- and low-pass filtering, was applied to recognize shallow and deep magnetic sources responsible for residual and regional anomalies. This approach effectively separates regional from residual signals, consistent with filtering theory [37]. The Gaussian high-pass filter emphasizes deeper (subsurface) anomalies, revealing MI values ranging from -289.8 to 66.2 nT (Figure 5). Green to blue zones (-289.8 to -50.2 nT) dominate the NE part of the study area, while yellow to pink zones (-44.5 to 66.2 nT) dominate the SW–SE portion. The modeling (Figure 5) recognized hidden anomalies at depths of 100 m to 1 km below the surface, supporting earlier findings on Gaussian filtering efficiency in anomaly separation [36].

3.1.2 Reduction to Pole (RTP) at low latitude

The RTP map (Figure 6), generated using Oasis Montaj, shows anomalies more directly above their causative sources by correcting for latitude effects on magnetic inclination. Magnetic intensity values range from 169.6 to -201.8 nT. High MI zones (-48.6 to 169.6 nT) dominate the NW, S, and SW portions of the study area, while low MI zones (-52.8 to -201.8 nT) are concentrated in the north and central parts. The magnetic high-to-low ratio is approximately 60: 40. RTP correction at low latitudes is critical for accurate anomaly positioning, as emphasized by Salem et al. [38].

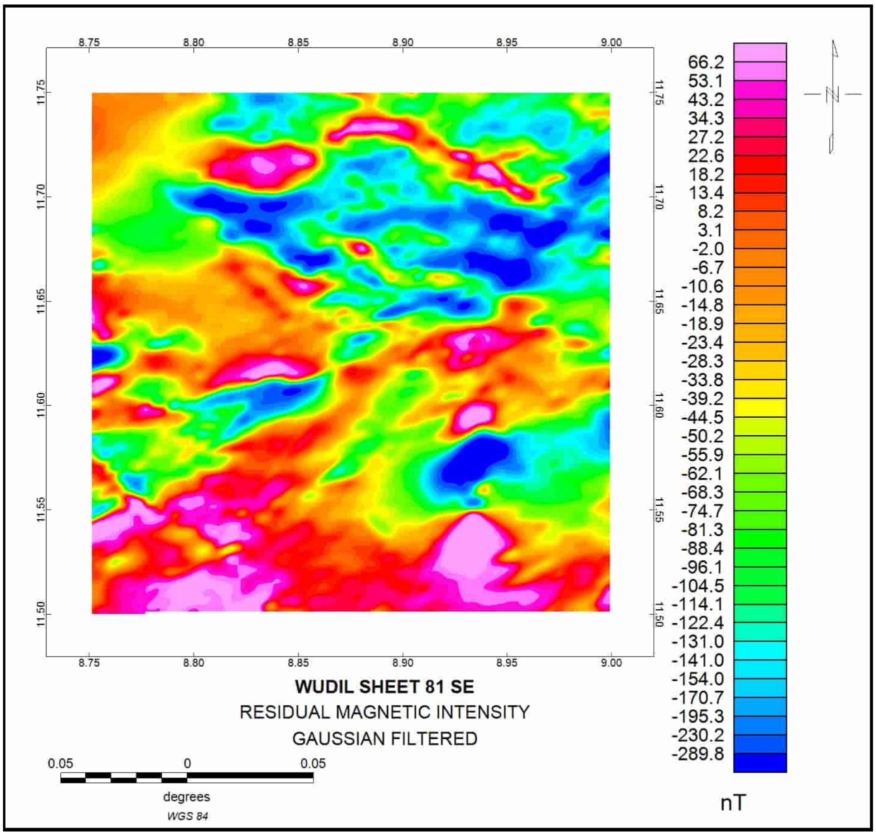

Figure 5. Residual magnetic intensity gaussian filtered from Wudil Sheet 81S

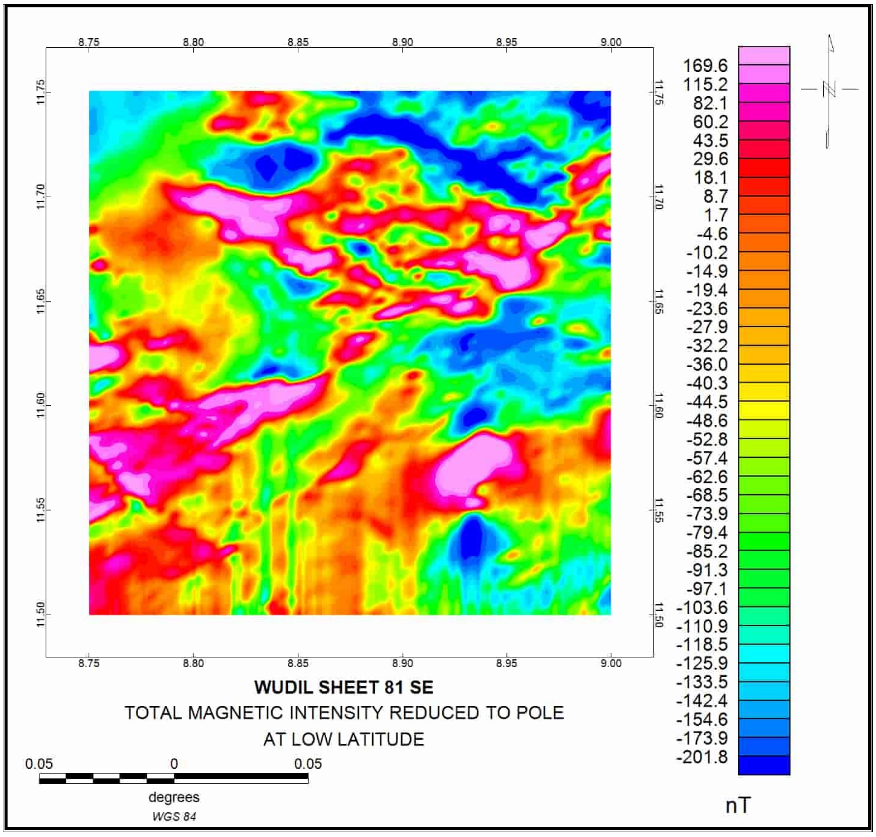

Figure 6. TMI reduced to pole at low latitude from Wudil Sheet 81SE

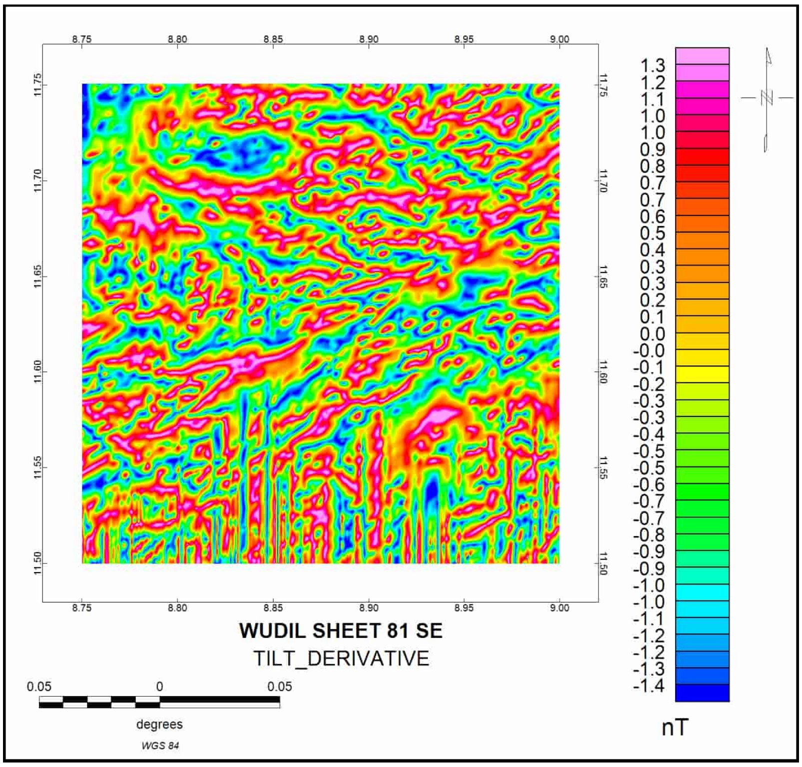

Figure 7. Tilt Derivative from Wudil Sheet 81 SE

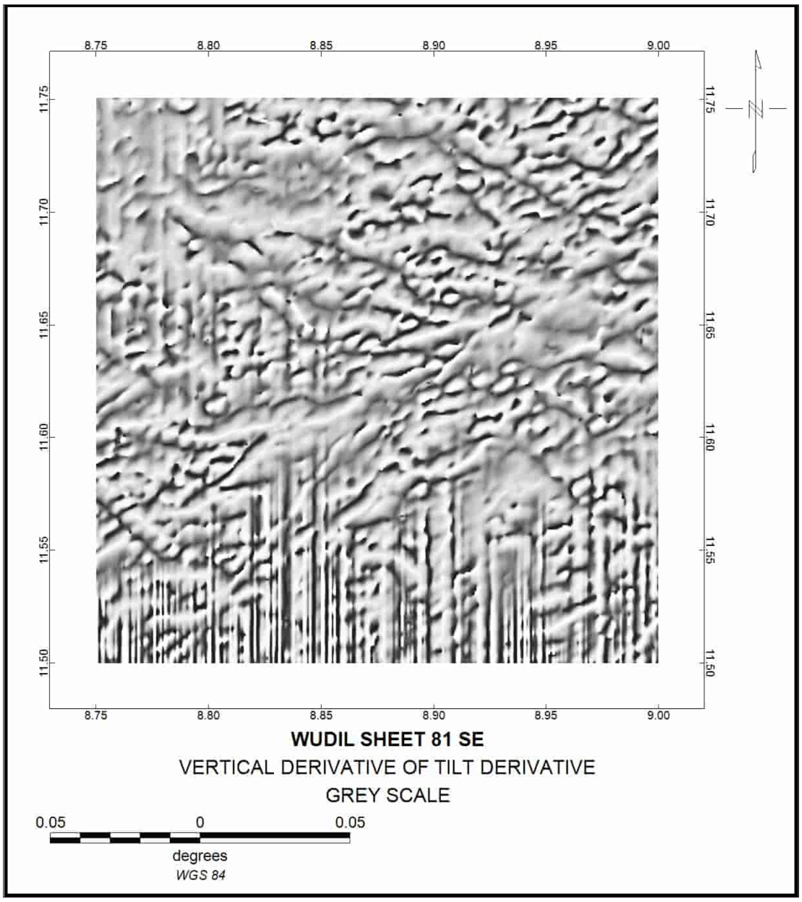

Figure 8. Vertical Derivative of Tilt Derivative (Grey Scale) from Wudil Sheet 81 SE

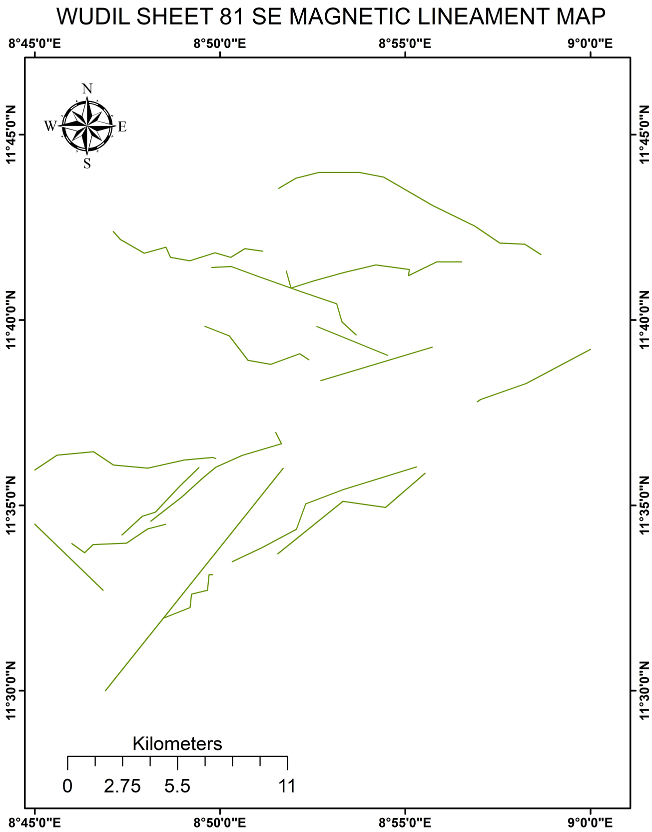

Figure 9. Magnetic lineament distribution map of Wudil Sheet 81 SE (TDR derivative-based)

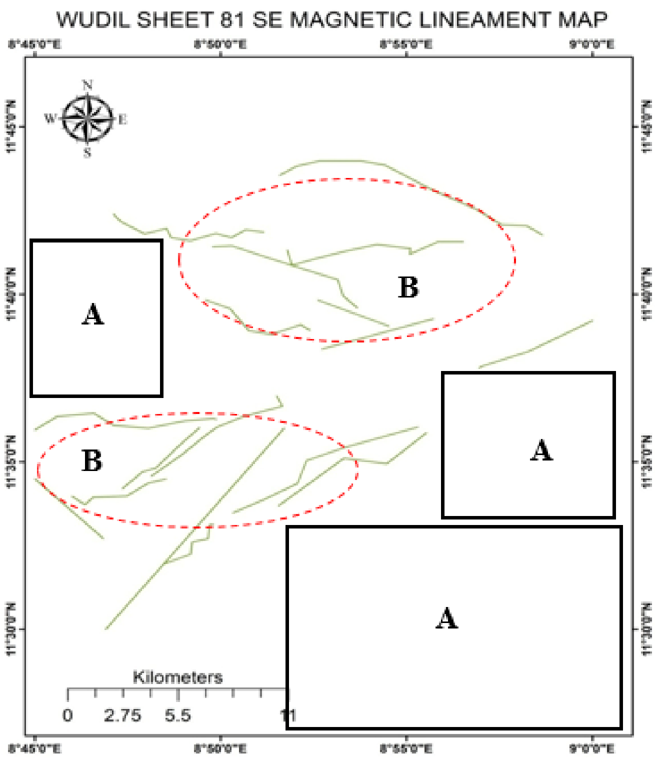

Figure 10. Magnetic lineament orientation rose diagram of Wudil Sheet 81 SE (Tectonic & dam-site analysis)

3.1.3 Tilt Derivative (TDR)

The Tilt Derivative (TDR) map (Figure 7) was generated from RTP data to enhance shallow structural edges. TDR effectively maps magnetic contacts and highlights short-wavelength anomalies, confirming its reliability in detecting near-surface structures [38, 39]. The intensity ranges from 1.3 to -1.4 nT/km, with high anomalies (-0.1 to 1.3 nT) in yellow to pink, and low anomalies (-1.4 to -0.2 nT) in blue to green. Unlike the RTP map, deep sources are suppressed, allowing only shallow structures to be imaged clearly.

The FVD map (Figure 7) highlights anomalies along the x-direction, especially in the central and SW parts of the study area. Derivative filters enhance edge detection by suppressing regional trends and emphasizing shallow features, consistent with SEG's [40] insights on linear feature analysis in aeromagnetic data.

3.1.4 Vertical Derivative of Tilt Derivative (Greyscale)

The Vertical Derivative of the TDR map (Figure 8) further enhances shallow structures, producing clearer delineation of lineaments and lithological boundaries. This method highlights subtle features not visible in the TMI or RTP maps, confirming findings in previous structural mapping studies [39].

3.1.5 Magnetic lineament map

The Magnetic lineament map (Figure 9) was manually extracted from the TDR derivative greyscale image (Figure 4). Lineaments are concentrated in the central part of Wudil Sheet 81 SE, while the SE and SW parts contain fewer lineaments. This observation aligns with SEG [40] studies showing how linear feature analysis can reveal fault and fracture orientations from aeromagnetic datasets.

3.2 Rose Diagram

The rose diagram for the Garko area reveals two dominant lineament trends: ENE–WSW and WNW–ESE. The ENE–WSW orientation is the most prominent and reflects the major tectonic fabric imposed during the Pan-African Orogeny (600 Ma), which shaped the structural architecture of the Nigerian Basement Complex [15, 18]. These lineaments represent long, persistent fractures and shear zones that influence groundwater flow and the mechanical stability of bedrock, making them key considerations in dam-site evaluation (Figure 10).

The WNW–ESE trend, although secondary, indicates younger tectonic reactivation superimposed on the Pan-African structures. These fractures are generally associated with brittle deformation and possible intraplate stress reactivation [17, 19]. The cross-cutting relationship between ENE–WSW and WNW–ESE lineaments suggests that the area has undergone multiple phases of deformation, resulting in a complex fracture network that can enhance secondary permeability.

From a dam construction perspective, areas where these lineaments intersect densely are structurally weaker and more susceptible to seepage, reducing foundation stability [41, 42]. In contrast, zones with sparse or widely spaced lineaments, particularly where ENE–WSW features dominate without significant WNW–ESE intersections, are more stable and suitable for dam foundations, highlighting the importance of rose diagram analysis in geotechnical planning.

3.3 Comparative Analysis of Filtering Techniques

A comparative evaluation of the TMI, RTE, FVD, and AS maps demonstrates varying levels of reliability and structural clarity. The RTE correction effectively repositioned anomalies but lacked sensitivity to shallow features. The FVD filter significantly enhanced near-surface structures but introduced noise, complicating interpretation in some regions. The AS map proved the most robust and internally consistent, offering stable anomaly enhancement and reliable structural edge detection. When anomalies appeared consistently across multiple filters, particularly RTE, FVD, and AS, they were classified as high-confidence structures. Minor fractures visible only on the FVD map, but absent on AS and RTE, were treated with caution due to potential derivative-induced noise. This approach aligns with recommended geophysical interpretation methodology, where multi-filter validation is essential for reducing uncertainty and improving geological accuracy [29, 43–45].

3.4 Structural Trends Identified

The integrated interpretation of the filtered magnetic maps revealed dominant structural orientations trending NE–SW, NW–SE, and subordinate E–W directions. The NE–SW trends correspond to Pan-African tectonic deformation, while the NW–SE structures are associated with later reactivations that affected large parts of the Nigerian Basement Complex. These lineaments represent fractures, faults, and lithological boundaries that control groundwater flow and basement competence. Zones with dense lineament intersections indicate structurally weakened regions and are considered unsuitable for dam foundations. In contrast, structurally homogeneous areas with minimal lineament density are more stable and favorable for dam construction.

3.5 Identification of Suitable Zones for Dam Construction

By integrating lineament density maps, structural consistency across filters, and magnetic susceptibility contrasts, two main zones emerged as suitable for dam development within the Garko area. These zones are characterized by low-to-moderate lineament density, dominance of high-susceptibility basement rocks, minimal evidence of fracturing, and consistent structural definition across AS, FVD, and RTE outputs.

Areas with intense fracturing, magnetic lows, or inconsistent filter signatures were excluded due to potential leakage pathways, reduced mechanical strength, or uncertain geological conditions. The identified zones therefore represent the most structurally competent and geophysically stable locations for dam foundation placement.

3.6 Lineament Identification Criteria

To ensure objective and reproducible structural interpretation for dam-site assessment in the Garko area, specific quantitative criteria were applied during lineament extraction. A minimum lineament length of 500 meters was set to focus on persistent fractures, faults, or lithological contacts that significantly influence rock stability and groundwater flow. Shorter features were only considered if consistently observed across multiple filtered datasets, ensuring the inclusion of shallow but geologically relevant structures [46–51].

Lineaments were grouped based on orientation trends into NE–SW, NW–SE, E–W, and N–S classes, with NE–SW and NW–SE being dominant. This classification helps distinguish major tectonic trends associated with the Pan-African Orogeny and subsequent reactivation events from minor or noise-related alignments. In addition, lineament density was assessed on a 1 km × 1 km grid and categorized into low, moderate, and high-density zones, linking fracture intensity to engineering suitability. Low-density areas were considered most favorable for dam foundations, while high-density zones were deemed structurally unstable [41, 42].

To validate the identified lineaments, only features appearing in two or more filtered magnetic outputs, including reduction to the equator, FVD, analytical signal, or upward/downward continuation maps, were considered reliable. This multi-filter consistency criterion reduced noise-induced artifacts and ensured structural relevance [29, 43]. Consequently, areas with long, coherent lineaments and low density were classified as most suitable for dam construction, whereas regions with intersecting major trends or high density were excluded due to increased risk of seepage and foundation instability.

4 Discussion

The aeromagnetic analysis of the Garko area demonstrates clear structural controls on dam-site suitability. The integration of TMI, Gaussian, RTP, Tilt Derivative, and Vertical Derivative filtering allowed the identification of major lineaments and subsurface structures. The dominant ENE–WSW and WNW–ESE trends observed in the rose diagram align with Pan-African tectonic fabrics, indicating that fracture density and orientation strongly influence both rock stability and groundwater flow. Areas with high lineament density, particularly where intersecting trends occur, were excluded from consideration due to their increased risk of seepage and foundation instability. Quantitative analysis suggests that regions with lineament densities above 12–15 km/km^2 and magnetic anomalies less than -0.3 nT should be considered unsuitable, whereas zones with densities below 5 km/km^2 and low to moderate magnetic variation (-0.3 to 0.4 nT) represent structurally stable foundations suitable for dam construction.

The depth sensitivity of the filtering methods significantly influenced the interpretation outcomes. The Gaussian high-pass filter highlighted deeper anomalies (100 m – 1 km) associated with major basement structures, while the Tilt Derivative and Vertical Derivative filters enhanced shallow structures ($<$100 m) controlling near-surface stability. This multi-scale approach allowed differentiation between deep-seated faults and surface fractures, reducing the risk of over interpretation. Nevertheless, some uncertainty remains due to the 500 m line spacing of the aeromagnetic survey and potential errors in depth estimation, which could slightly shift the interpreted locations of faults and fractures. To mitigate this, geological and field validation through boreholes, trenching, or surface lithology comparison is recommended before final dam construction.

From a geotechnical and socio-economic perspective, the identified zones are accessible by existing motorable roads and footpaths, making construction logistics feasible. The stable southern and northern areas around Garfa, Sarina, Sumaila, Utai, and Sayasaya also coincide with regions of seasonal water accumulation, supporting irrigation, domestic water supply, and flood control. Excluded unsuitable zones, mainly in the central portion of the study area, exhibit dense intersecting lineaments, low magnetic intensities, and potential water leakage pathways, which would compromise both structural integrity and water retention. By combining geophysical interpretation with structural and hydrological reasoning, this study provides a practical framework for selecting dam sites that balance engineering stability, resource availability, and social utility.

5 Conclusion

Aeromagnetic investigations of Wudil Sheet 81 SE using TMI, RTP, Gaussian, Tilt Derivative, and lineament analyses identified key structural controls relevant to dam-site selection. Two main zones were delineated based on magnetic intensity and fracture density. Structurally stable zones, suitable for dam foundations, are characterized by low lineament density ($\leq$2 lineaments/km^2) and moderate magnetic intensity (-0.3 to 0.4 nT/km in Tilt Derivative maps). These zones are predominantly located in the southern and northern parts of the study area, including Garfa, Sarina, Sumaila, Utai, Sayasaya, and parts of Garko.

Conversely, structurally unstable zones, which are unsuitable for dam construction, display high lineament density ($>$2 lineaments/km^2) and extreme magnetic values ($<$-0.3 nT/km or $>$0.4 nT/km), particularly where NE–SW and WNW–ESE fractures intersect. These areas, concentrated in the central portion of the study area, present higher risks of seepage, reduced mechanical strength, and foundation instability.

This study demonstrates that integrating multi-filter aeromagnetic processing with quantitative lineament mapping provides reliable criteria for preliminary dam-site assessment. The established thresholds offer practical guidance for engineering decision-making, though field verification and detailed geotechnical investigations remain essential to confirm structural suitability and ensure long-term stability of dam foundations.

Author Contributions

Conceptualization, M.A. and M.A.A.; methodology, M.A.; software, M.A.; validation, M.A., M.A.A., R.T.D., and A.M.; formal analysis, M.A.; investigation, M.A.; resources, M.A.A. and A.M.; data curation, M.A.; writing original draft preparation, M.A.; writing review and editing, M.A., M.A.A., R.T.D., and A.M.; visualization, M.A.; supervision, M.A.A.; project administration, M.A. All authors have read and agreed to the published version of the manuscript.

Data Availability

The data used to support the findings of this study are available from the corresponding author upon request.

Conflicts of Interest

The authors declare that they have no conflicts of interest.

References

[1] M. H. Al-Kubaisi and Q. Y. Al-Kubaisi, "Selection of dam sites for rainwater harvesting in Western Desert of Iraq: A case study in Wadi Al-Mohammadi Basin," *Iraqi Geol. J.*, vol. 56, no. 1F, pp. 38–50, 2023. https://doi.org/10.46717/igj.56.1F.3ms-2023-6-11

[2] Iberdrola, "Geological surveys: Keys to dam engineering," 2023. https://www.iberdrola.com/about-us/what-we-do/hydro-electric-energy/geological-study

[3] GeoFEM, "The role of geology in dam site selection," 2022. https://www.geofem.com/post/the-role-of-geology-in-dam-site-selection

[4] Y. Wang, Y. Tian, and Z. Cao, "Dam siting: A review," *Water*, vol. 13, no. 15, p. 2080, 2021. https://doi.org/10.3390/w13152080

[5] P. Sentenac, V. Benes, and H. Keenan, "Reservoir assessment using non-invasive geophysical techniques," *Environ. Earth Sci.*, vol. 77, no. 16, p. 293, 2018. https://doi.org/10.1007/s12665-018-7463-x

[6] Wikipedia Contributors, "Electrical resistivity tomography," 2024. https://en.wikipedia.org/wiki/Electrical_resistivity_tomography

[7] A. Aina, M. O. Olorunfemi, and J. S. Ojo, "An integration of aeromagnetic and electrical resistivity methods in dam site investigations," *Geophysics*, vol. 61, no. 2, pp. 349–356, 1996. https://doi.org/10.1190/1.1443963

[8] O. V. Fatoye, S. A. Adebayo, J. K. Ayeni, and J. O. Ibiwoye, "Subsurface geology and structural trend evaluation of dam using multi-techniques," *Discover Geosci.*, vol. 3, no. 1, p. 39, 2025. https://doi.org/10.1007/s44288-025-00149-y

[9] F. F. Katty, B. A. Ankidawa, G. I. Obiefuna, Y. B. Valdon, and I. A. Kwami, "A proposed dam site investigation using integrated geophysical and geotechnical methods; A case study of Loko area, Northeastern Nigeria," *Glob. J. Geol. Sci.*, vol. 22, no. 1, pp. 31–45, 2024. https://doi.org/10.4314/gjgs.v22i1.3

[10] Nigerian Meteorological Agency (NIMET), "Climate review bulletin for Northern Nigeria," Abuja, Nigeria, 2020. https://nimet.gov.ng/publication

[11] E. A. Olofin, "Human and environmental aspects of Kano region," 1987. https://bucore.buk.edu.ng

[12] A. S. Aliyu, "Geological and structural studies of Garko area, Kano state, Northwestern Nigeria," Master's thesis, Department of Geology, Ahmadu Bello University, Zaria, Nigeria, 2005, unpublished M.Sc. Thesis. https://www.abu.edu.ng/theses

[13] Nigerian Geological Survey Agency (NGSA), "Geological map of Nigeria, Sheet 81 (Wudil SE)," Abuja, Nigeria, 2006. https://www.ngsa.gov.ng/publications/maps

[14] J. O. Ayoade, *Introduction to Hydrology*. Ibadan, Nigeria: Spectrum Books Limited, 2011. https://www.worldcat.org/title/introduction-to-hydrology/761632097
[15] A. C. Ajibade, M. A. Rahaman, and A. E. Ogezi, "The precambrian of Nigeria," in *Geology of Nigeria*, Jos, Nigeria, 1987, pp. 57–68. https://www.worldcat.org/title/geology-of-nigeria/754663525
[16] P. McCurry, "The geology of the precambrian to lower palaeozoic rocks of Northern Nigeria – A review," in *Geology of Nigeria*, Lagos, Nigeria, 1976, pp. 15–39. https://search.worldcat.org/title/geology-of-nigeria/ocl c/6791305
[17] U. A. Danbatta and A. Garba, "Lineament mapping and groundwater exploration in the basement complex terrain of Kano state, Northwestern Nigeria," *J. Appl. Sci. Environ. Manag.*, vol. 15, no. 2, pp. 297–303, 2011. https://doi.org/10.4314/jasem.v15i2.7
[18] M. A. Rahaman, "Recent advances in the study of the basement complex of Nigeria," in *Pre Cambrian Geology of Nigeria*, 1988, pp. 11–41.
[19] N. G. Obaje, *Geology and Mineral Resources of Nigeria*. Berlin: Springer, 2009. https://doi.org/10.1007/978-3-540-92685-6
[20] I. B. Odeyemi, M. A. Rahaman, and O. O. Ocan, "Geology and geochemistry of the Nigerian schist belts," in *Geology of Nigeria (2nd ed.)*. Rock View (Nigeria) Limited, Lagos, Nigeria, 1999, pp. 141–156.
[21] Nigerian Geological Survey Agency (NGSA), "Geological and mineral resources map of Kano state, Nigeria," Abuja, Nigeria, 2011. https://www.ngsa.gov.ng/publications/maps
[22] Nigerian Geological Survey Agency (NGSA), "High resolution aeromagnetic data of Nigeria," Abuja, Nigeria, 2009. https://www.ngsa.gov.ng/publications/maps
[23] Geosoft, *Oasis Montaj Geophysical Mapping and Processing System: User Guide*, Toronto, Canada, 2019. https://www.geosoft.com/resources/manuals
[24] J. D. Philips, "Geosoft eXecutables (GX's) developed by the US Geological Survey," 2007, 2007-1355. https://doi.org/10.3133/ofr20071355
[25] B. M. Geographics, *Global Mapper User Guide*, Hallowell, Maine, USA, 2020. https://www.bluemarblegeo.com/products/global-mapper.php
[26] Environmental Systems Research Institute (ESRI), *ArcGIS Desktop: Release 10.8 Documentation*, Redlands, CA, USA, 2020. https://desktop.arcgis.com/en/documentation/
[27] W. J. Hinze, R. R. B. Von Frese, and A. H. Saad, *Gravity and Magnetic Exploration: Principles, Practices, and Applications*. Cambridge University Press, 2013.
[28] P. Kearey, M. Brooks, and I. Hill, *An Introduction to Geophysical Exploration*. John Wiley & Sons, 2002.
[29] M. Dentith and S. T. Mudge, *Geophysics for the Mineral Exploration Geoscientist*. Cambridge University Press, 2014. https://doi.org/10.1017/CBO9781139024358
[30] J. M. Reynolds, *An Introduction to Applied and Environmental Geophysics*. John Wiley & Sons, 2011.
[31] W. M. Telford, L. P. Geldart, and R. E. Sheriff, *Applied Geophysics*. Cambridge University Press, 1990.
[32] P. V. Sharma, *Environmental and Engineering Geophysics*. Cambridge University Press, 1997.
[33] D. A. Clark, "Magnetic petrophysics and magnetic petrology: Aids to geological interpretation of magnetic surveys," *AGSO J. Aust. Geol. Geophys.*, vol. 17, no. 2, pp. 83–103, 1997.
[34] A. Biswas and S. P. Sharma, "Interpretation of aeromagnetic data using Euler deconvolution and its practical applications," *J. Appl. Geophys.*, vol. 131, pp. 122–134, 2016. https://doi.org/10.1016/j.jappgeo.2016.06.004
[35] O. O. Ocan, M. A. Oladunjoye, and M. Alaba, "Lineament mapping and groundwater exploration using aeromagnetic data of Iwaraja area, Southwestern Nigeria," *Ife J. Sci.*, vol. 15, no. 2, pp. 351–361, 2013. https://science.oauife.edu.ng/ife-journal-of-science/
[36] M. A. Fkirin, M. A. S. Youssef, and M. F. El-Deery, "Prediction of aeromagnetic system based on digital filters by MATLAB and Oasis Montaj software," *WSEAS Trans. Signal Process.*, vol. 15, no. 2, pp. 1–8, 2019.
[37] Wikipedia Contributors, "Gaussian filter," 2025. https://en.wikipedia.org/wiki/Gaussian_filter
[38] A. Salem, S. Williams, J. D. Fairhead, D. Ravat, and R. Smith, "Tilt-depth method—A simple depth estimation method using first-order magnetic derivatives," *Geophys. J. Int.*, vol. 171, no. 2, pp. 705–716, 2007. https://doi.org/10.1111/j.1365-246X.2007.03550.x
[39] D. Knaust, "The ichnogenus Ophiomorpha: Taxonomy and environmental distribution," *Earth-Sci. Rev.*, vol. 261, p. 104988, 2024. https://doi.org/10.1016/j.earscirev.2024.104988
[40] R. O. Hansen and E. deRidder, "Linear feature analysis for aeromagnetic data," *Geophysics*, vol. 71, no. 6, pp. L61–L67, 2006. https://doi.org/10.1190/1.2357831
[41] C. R. Twidale and E. M. Campbell, "Fractures and rock mechanics in geomorphology," *Geomorphology*, vol. 6, no. 1, pp. 51–71, 1993. https://doi.org/10.1016/0169-555X(93)90027-6
[42] B. Singh and R. K. Goel, *Engineering Rock Mass Classification*. Boston: Butterworth-Heinemann, 2011.

[43] M. N. Nabighian, “The analytic signal of two-dimensional magnetic bodies with polygonal cross-section: Its properties and use for automated anomaly interpretation,” *Geophysics*, vol. 37, no. 3, pp. 507–517, 1972. https://doi.org/10.1190/1.1440276

[44] A. B. Reid, J. M. Allsop, H. Granser, A. T. Millett, and I. W. Somerton, “Magnetic interpretation in three dimensions using Euler deconvolution,” *Geophysics*, vol. 55, no. 1, pp. 80–91, 1990. https://doi.org/10.1190/1.1442774

[45] X. Li, “Understanding 3D analytic signal amplitude,” *Geophysics*, vol. 71, no. 2, pp. L13–L16, 2006. https://doi.org/10.1190/1.2184367

[46] D. W. O’Leary, J. D. Friedman, and H. A. Pohn, “Lineament, linear, lineation: Some proposed new standards for old terms,” *Geol. Soc. Am. Bull.*, vol. 87, no. 10, pp. 1463–1469, 1976.

[47] K. Koike, T. Yoshinaga, and W. F. Panton, “Lineament analysis using satellite imagery,” *Int. J. Remote Sens.*, vol. 19, no. 1, pp. 19–42, 1998. https://doi.org/10.1080/014311698215308

[48] S. O. Ariyo and A. Yusuf, “Hydrogeological assessment of Hadejia–Jama’are Basin, Northern Nigeria,” *J. Water Resour. Eng.*, vol. 4, no. 2, pp. 45–56, 2013. http://www.jwre.org/vol4/issue2/ariyo2013

[49] M. A. Lawal, A. O. Oshomoji, A. A. Akinlalu, K. O. Omosanya, O. S. Ndukwe, K. A. N. Adiat, and G. O. Mosuro, “A simplified GIS and Google Earth based approach for lineaments and terrain attributes mapping in a basement complex terrain,” *Sci. Rep.*, vol. 12, no. 1, p. 15801, 2022. https://doi.org/10.1038/s41598-022-20057-2

[50] A. A. Fatoyinbo, K. S. Ishola, C. J. Okolie, O. E. Daramola, I. A. HamidMosaku, O. A. Ipadeola, and S. E. Erharhaghen, “Integration of geospatial and geophysical data for assessing borehole conditions at the University of Ilorin, North-Central, Nigeria,” *Nigerian J. Technol.*, vol. 38, no. 1, pp. 144–153, 2019. https://doi.org/10.4314/njt.v43i3.19

[51] J. B. Wright, D. A. Hastings, W. B. Jones, and H. R. Williams, *Geology and Mineral Resources of West Africa*. London, UK: George Allen & Unwin, 1985, vol. 187. https://link.springer.com/book/10.1007/978-94-015-3932-6